

Northumbria Research Link

Citation: Kavungal, Vishnu, Farrell, Gerald, Wu, Qiang, Mallik, Arun Kumar and Semenova, Yuliya (2018) A comprehensive experimental study of whispering gallery modes in a cylindrical microresonator excited by a tilted fiber taper. *Microwave and Optical Technology Letters*, 60 (6). pp. 1495-1504. ISSN 0895-2477

Published by: Wiley-Blackwell

URL: <https://doi.org/10.1002/mop.31186> <<https://doi.org/10.1002/mop.31186>>

This version was downloaded from Northumbria Research Link:
<http://nrl.northumbria.ac.uk/34271/>

Northumbria University has developed Northumbria Research Link (NRL) to enable users to access the University's research output. Copyright © and moral rights for items on NRL are retained by the individual author(s) and/or other copyright owners. Single copies of full items can be reproduced, displayed or performed, and given to third parties in any format or medium for personal research or study, educational, or not-for-profit purposes without prior permission or charge, provided the authors, title and full bibliographic details are given, as well as a hyperlink and/or URL to the original metadata page. The content must not be changed in any way. Full items must not be sold commercially in any format or medium without formal permission of the copyright holder. The full policy is available online: <http://nrl.northumbria.ac.uk/policies.html>

This document may differ from the final, published version of the research and has been made available online in accordance with publisher policies. To read and/or cite from the published version of the research, please visit the publisher's website (a subscription may be required.)

www.northumbria.ac.uk/nrl



A comprehensive experimental study of whispering gallery modes in a cylindrical micro-resonator excited by a tilted fiber taper

Vishnu Kavungal^{1*}, Gerald Farrell¹, Qiang Wu^{1,2}, Arun Kumar Mallik¹, and Yuliya Semenova¹

¹ Photonics Research Centre, Dublin Institute of Technology, Kevin St, Dublin, Ireland

²Department of Mathematics, Physics and Electrical Engineering, Faculty of Engineering and Environment, Northumbria University, Newcastle upon Tyne, NE1 8ST, United Kingdom

*Corresponding author: vishnu.kavungal@mydit.ie

ABSTRACT

Whispering gallery modes (WGMs) excitation in a cylindrical micro-resonator formed by a section of silica optical fiber has been studied. Evanescent light coupling into the micro-resonator is realized using a tapered optical fiber, fabricated by a micro-heater brushing technique. Several types of silica fibers with different diameters are studied as micro-resonators, and the influence of the resonator's diameter on the excitation of WGMs is investigated. The excitation of WGMs in a cylindrical fiber resonator were studied with changes to the tilt angle between the micro-cylinder and the fiber taper in the range of angles from a perpendicular position (0°) to large tilt angles (24°). The evolution of the fiber taper transmission spectrum with the change of the tilt angle results in changes in the intensity, broadening of and a blue shift in the WGM resonance spectra. Overall losses in the taper transmission spectrum decrease with the increase of the taper tilt angle from its perpendicular position, followed by a complete disappearance of the WGM resonances at large tilt angles greater than 20° .

Keywords: Whispering gallery modes; Tapered fiber; Microcavities; Optical microresonators; Fiber optic sensors

I. INTRODUCTION

Whispering gallery modes (WGMs) are electromagnetic surface oscillations formed in dielectric micro resonators with a circular structure such as spheres, cylinders or disks. WGMs arise as a result of trapping of light within the micro resonator by total internal reflections from the resonator's curved surface. Such reflections force the light to take on a polygonal path within the curved structure, effectively confining its energy to a very small volume.

Optical micro-resonators supporting WGMs are attractive photonic devices due to their small mode volumes, very high power densities, narrow spectral linewidths and high Q factors. Such micro-resonators have been shown to have potential use in many areas, including studies of nonlinear optical effects and quantum electrodynamics, low threshold micro-lasers and very sensitive micro-sensors. WGMs can be supported by a variety of resonator geometries and the choice of the particular resonator for a given application is usually influenced by three major factors: the achievable value of the Q -factor; ease of fabrication and ease of integration [1-4]. The most common micro resonators are spherical; they are relatively easy to fabricate and usually have very high Q -factors: $\sim 10^9$ at $1.55 \mu\text{m}$ for silica [5] and $\sim 10^5$ at $1.55 \mu\text{m}$ for chalcogenide glass [6].

Cylindrical WGM resonators have the disadvantage that due to the longitudinal degree of freedom in such structures a coupled beam can spread along the cylinder length and eventually vanish even if there is no material loss. However, Sumetsky et al. [7] theoretically reported an infinitely long cylindrical micro-resonator with its Q -factor as high as that of spherical and spheroid counterparts.

There are a number of potential advantages that make fiber-based cylindrical resonators worth exploring. Some of these have been pointed out previously by Farca *et al.* [8]: optical fibers are highly uniform in diameter, allowing large numbers of identical resonators to be fabricated easily and providing a high degree of repeatability; fiber micro cylinders are easy to handle, and the alignment for optimal coupling of the excitation light into the fiber resonator depends on only one angular degree of freedom, as opposed to two for experiments involving microspheres. Due to this the optical setup for fiber-based experiments is more straightforward. Moreover, previously reported experiments showed that micro-cylindrical resonators demonstrate narrow peaks for both the microfiber taper/micro-cylinder configuration [9] and for free Gaussian beam scattering [10]. The authors in [11-13] demonstrated that excitation of WGMs in cylindrical fiber resonators can be applied to high-resolution measurements of the fiber diameter variations. More recently, authors in [14] reported a tunable high Q -factor cylindrical micro resonator based on a tapered silica micro-fiber.

There are several methods of light coupling in and out of a WGM resonator, that includes free space coupling and guided wave coupling. In free space coupling WGMs are excited using focused lased pump to the resonator and the transmitted light is collected using a collimator to a detector [15-17]. In guided wave coupling, the most commonly used method is based on

evanescent-wave coupling either from an adjacent guiding structure such as a tapered optical fiber coupler, a polished fiber half block coupler [18, 19] or a channel waveguide coupler [20], and coupling under frustrated total internal reflections such as a prism [21] or an angle-polished fiber [22]. Among them tapered fiber is an excellent and easy to align coupling approach with a demonstrated ultra-high coupling efficiency of up to 99% [23]. The phase matching condition in the tapered fiber coupling can also be controlled by the diameter of the taper and the gap between the fiber taper and the resonator [24].

In order to maintain stable coupling conditions and to protect the micro resonator-tapered fiber system from environmental perturbations many techniques have been developed. These include packaging of the resonator-coupler system with a low refractive index UV curable [6, 25-27] and moisture curable [28] polymer glue, fabrication of silica side walls close to the resonator for mechanical support of the tapered fiber [27-29] and the use of special resonator shapes such as an inverted wedge silica resonator [29] and an octagonal silica toroid [30]. Maintaining perfect alignment of the light coupling tapered optical fiber and the micro-resonator during packaging is a challenging task since perturbations can lead to a misalignment or tilting of the tapered fiber with respect to the resonator.

Tilting, where the cylindrical micro-resonator is not perpendicular to the coupling fiber, has an effect on WGM excitation in a cylindrical micro-resonator. This was studied by J. A. Lock *et al.* [31, 32] and A. W. Poon *et al.* [10]. In their experiments, spiral morphology dependent resonances in an optical fiber were excited by elastic scattering of both focused and unfocused laser beams on a tilted optical fiber with small angles from perpendicular to the incident beam propagation directions. A. Boleininger *et al.* [13] reported an investigation of tilting effect of cylindrical micro-resonator on the excitation of WGMs by the evanescent field of a tapered optical fiber. However, in their work the range of tilt angles of the micro-resonator with respect to the perpendicular position of the tapered fiber was limited to 13° and several significant aspects of tilting, such as its influence on the overall transmission losses and resonance wavelength shift were not considered.

To the best of our knowledge this work is the first comprehensive experimental investigation of the influence of the fiber taper tilt on the excitation of WGMs in a fiber cylindrical micro-resonator. We report on changes in the evolution of the WGM transmission spectrum of the tapered fiber with the increase of the tilt angle between the fiber resonator and the taper in the range of tilt angles from the perpendicular position of the taper (0°) to 60° tilt angle and analyze the influence of the tilt on the spectral positions of the WGM resonances and the effect of tilting on light transmission in the taper.

In addition, we investigate and analyze the optimum fiber taper waist diameter to achieve the most efficient light coupling into the micro-resonator and the influence of the resonator radius on the parameters of the WGM spectrum, such as Q-factor and the free spectral range.

II. PROPERTIES OF WGM RESONANCES

WGM resonances excited in the cylindrical cavity can be characterized by their quality factor (Q), a figure of merit generally used to describe all kinds of resonators. In our case the WGM resonant modes are formed in the transmission spectrum of the tapered fiber due to the destructive interference between the light propagating in the tapered fiber and the light circulating inside the cylindrical cavity. The transmission spectrum of the fiber taper typically displays a periodic pattern of Lorentzian dips corresponding to the WGM resonances. The separation of successive resonances is referred as the free spectral range (FSR).

A simple approximation can be obtained for the FSR from the propagation constant, starting with [33, 34]

$$\frac{\partial\beta}{\partial\lambda} = \frac{-\beta}{\lambda} + k \frac{\partial n_{eff}}{\partial\lambda} \quad (1)$$

Neglecting the wavelength dependency of the refractive index [33] yields

$$\frac{\partial\beta}{\partial\lambda} = \frac{-\beta}{\lambda} + \frac{2\pi}{\lambda} \frac{\partial n_{eff}}{\partial\lambda} \approx \frac{-\beta}{\lambda} \quad (2)$$

The FSR of the resonator is then given by the equation:
$$FSR = \frac{-2\pi}{L} \left(\frac{\partial\beta}{\partial\lambda} \right)^{-1} = \frac{-2\pi}{L} \left(\frac{-\lambda}{\beta} \right) \approx \frac{\lambda^2}{n_{eff}L} \quad (3)$$

where L is the circumference of the resonator. Thus, the FSR is given by:

$$FSR = \frac{\lambda^2}{2\pi R_{eff} n_{eff}} \quad (4)$$

From this approximate relationship between the FSR and the radius of the resonator, it is clear that the WGMs spectral spacing decreases with an increase of the resonator radius and thus a larger cavity can accommodate a higher number of modes. The WGMs spectral positions follow a simple approximation:

$$\lambda_m = \frac{2\pi R n}{m} \quad (5)$$

where R is the radius of the resonator, n is the refractive index of the resonator, λ_m is the resonance wavelength and m is the integer called the azimuthal mode number. This approximation is more accurate when the path taken by the light is close to a circle, which is true for larger radius resonators. This is because, based on a ray optics model, the total internal reflection path around the curved surface is polygonal in nature, so the true path taken by the light is slightly shorter than the circumference of the resonator and thus the resonance wavelength is slightly shorter than the predicted by the Eq. (6) value [13].

Using a wave optics model one can get more accurate values for the resonance wavelength by solving the respective eigenvalue equation inside the cavity. WGMs in a cylindrical cavity are defined by three mode numbers: the radial mode number (l), the azimuthal mode number (m) and the slab mode number (p). For a WGM with a mode number m there are $2m$ field maxima around the circumference of the cylinder (cylinder azimuth), $(l-1)$ nodes along the radial coordinate of the cylinder and p nodes along the axis of the cylinder [13].

As stated above, the azimuthal mode number (m) is related to the number of field maxima distributed along the circumference of the resonator, so for a larger cylinder radius the azimuthal number of the resonant modes increases but this also leads to a reduction of the spectral spacing between the WGM resonances. Spectra with well separated WGMs are desirable for sensing applications, since in this case spectral shifts are easier to discern. Thus, for example, the authors in [35, 36] increased the FSRs of their sensors by reducing the diameter of the sensor structures.

The sharpness of the WGM spectral dips greatly impacts the resolution of sensors based on WGM micro-resonators, since a sharper peak allows for the detection of smaller spectral shifts in the resonance wavelength. This sharpness can be characterized by the value of Q-factor of the micro-resonator. The Q-factor is a dimensionless parameter related to loss of energy in an oscillatory system. It is defined as the ratio of the central resonance wavelength (λ_m) to the full width at half depth ($\Delta\lambda_m$) of the same resonance:

$$Q = \frac{\lambda_m}{\Delta\lambda_m} \quad (6)$$

In an resonant optical structure, the Q-factor is proportional to the decay time of the mode, which in turn is inversely related to the sum of losses from the various loss mechanisms. The quality factor in WGM resonators is limited by various factors such as intrinsic radiative (curvature) losses, scattering losses due to residual surface inhomogeneities, losses due to surface contaminants and material losses [37]. When WGMs in a resonator are excited using a tapered fiber in contact with the resonator, the corresponding Q-factor is referred to as a loaded Q-factor. Due to physical contact of the fiber taper, coupling will cause additional losses in the resonator. The unloaded or intrinsic Q-factor of the resonator is the Q-factor calculated in the absence of coupling losses. The loaded Q-factor is always smaller than the unloaded Q-factor [34].

III. EXPERIMENTAL ARRANGEMENT, RESULTS AND DISCUSSION

(a) Fabrication of tapered optical fibers

Light propagation inside a standard optical fiber with a diameter greater than the propagating light wavelength is guided by total internal reflection and the light is localized inside the core. When light hits the interface between the core and cladding layers, a small portion of the light energy infiltrates the cladding as an evanescent field that exponentially decays into the cladding region. The penetration depth of the evanescent field into the cladding is given by the formula [38]

$$d_p = \frac{\lambda}{2\pi(n_1^2 \sin^2 \theta - n_2^2)^{1/2}} \quad (7)$$

where λ is the wavelength of light and n_1 and n_2 are the refractive indices of the core and cladding respectively. θ is the incident angle measured from the normal at the interface of the core and cladding. The reflected beam from the interface is returned to the core with a phase shift along its axial propagation direction.

When the diameter of the optical fibre is greatly reduced to a micron scale by tapering, the original boundary between the fibre core and cladding at the waist region is no longer significant. The refractive index contrast between the core and cladding becomes very small. In this case, an optical microfiber can be considered as a cylindrical waveguide with a homogeneous refractive index profile. In a thin fiber taper light is guided by the total internal reflection at the cladding-air interface (if the surrounding medium is air). Under these conditions a significant portion of light propagates outside of the microfiber. The presence of a large evanescent field outside of the tapered portion of the fiber can be used for coupling the light into another fiber acting as the micro-cylinder by placing both fibers in direct physical contact.

The optical properties of the tapered micro-fibers strongly depend on the geometry of both their transition and waist regions. If the tapering process is carried out in such a way that the fiber diameter within its transition region changes smoothly and can be adiabatically slow as a function of fiber length, the taper is considered adiabatic. This condition ensures low transmission loss and small inter-mode coupling. In our experiments, we used adiabatic tapers for excitation of WGMs from cylindrical micro-resonators. [39, 40].

The fiber taper for light coupling was fabricated using the micro-heater brushing technique. A short length of a coating-stripped standard single mode fiber (SMF 28, Corning) with core and cladding diameters of 8.3 and 125 μm respectively was cleaned with isopropyl alcohol. The stripped and cleaned fiber section was fixed horizontally between two computer controlled XYZ translational stages. The tapered fiber was then fabricated by means of a customized micro-heater brushing technique described in [41]. A ceramic micro heater (CMH-7019, NTT-AT) was used to heat the fiber up to approximately 1300°C, making the silica material soft enough for tapering. A customized PC program allowed for an accurate control of the diameter, the length and the shape of the fabricated tapers.

In our experiment, the tapered waist diameter is approximately 1.3 μm , the waist length is around 3.5 mm and the full taper length is circa 30 mm. The fabricated fiber taper was then fixed on a glass slide at a height of ~ 1 mm from the slide surface using two drops of UV curable epoxy (Norrand). The total length of the fiber between the cured epoxy droplets was 40 mm. Figure 1 shows the schematic diagram of the optical fiber tapering setup.

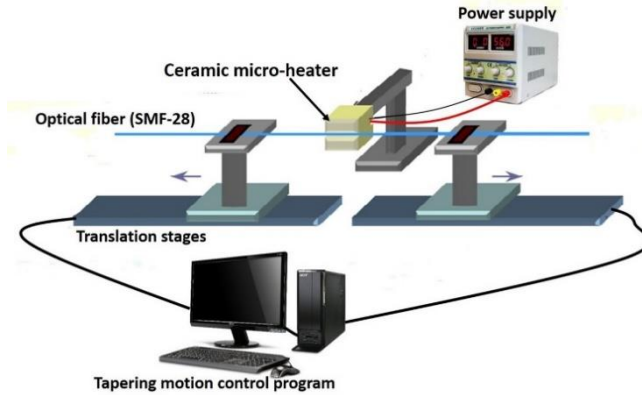


Fig. 1. Schematic diagram of the microfiber fabrication setup based on the microheater brushing technique.

The fabricated fiber taper with waist diameter of circa ~ 1.3 μm was experimentally determined to be the optimal diameter choice to balance the need for effective light coupling against mechanical fragility. Initially the transmission loss of the tapered fiber was measured as a function of wavelength, with reference to the un-tapered fiber. It was found that the fiber taper shows an increased 1.3 dB loss over the spectral range from 1500 to 1600 nm, compared with the un-tapered fiber.

(b) Experimental setup

In our experiment a short (circa 3 cm) section of a silica optical fiber with its buffer coating removed using a fiber stripper was used as the micro-cylinder. Evanescent light coupling to the micro-cylinder was achieved by a full fiber taper placed in physical contact with the micro-cylinder. Figure 2 illustrates schematically the experimental setup for recording the transmission spectrum of the micro-fiber taper and observation of the WGMs of the cylindrical micro-resonator.

The input end of the fiber taper was connected to a Super luminescent diode (SLD) (Thorlabs), with a wavelength range of 1500-1600 nm followed by a three-paddle manual polarization controller (Thorlabs). The output of the fiber taper is connected to an Optical Spectrum Analyser (OSA) (86142B, Agilent).

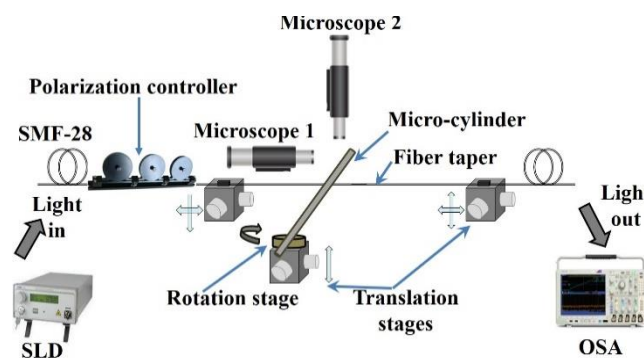


Fig. 2. Experimental setup for observation of the transmission spectrum of WGMs in a cylindrical micro-resonator excited by a fiber taper.

Figure 3 is a microphotograph of the micro-cylinder resonator in perpendicular position with respect to the tapered fiber. Here Z_{fiber} is the micro-cylinders meridional axis with the laboratory coordinates system (X_{lab} ; Z_{lab}), X_{lab} is the axis of the tapered fiber and Z_{lab} is the normal to the tapered fiber.

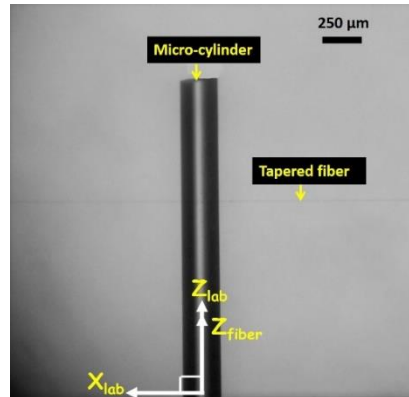


Fig. 3. microphotograph of the micro-cylinder resonator in perpendicular position with respect to the tapered fiber.

(c) Selection of the optimal tapered fiber diameter

For selecting the optimum tapered fiber diameter for the excitation of WGMs for a particular diameter microcylinder, fine tuning of the phase matching was performed by moving the microcylinder along the taper relative to the waist region while keeping both the micro-cylinder and tapered fiber perpendicular relative to each other.

Figure 4 shows the WGM spectra recorded by placing a 240 μm cylindrical micro-resonator in direct contact with a tapered fiber at different positions along its axial direction corresponding to the varying diameters of the taper waist region. The waist diameter of the fabricated tapered fiber at its thinnest part is circa $\sim 1.3 \mu\text{m}$. It can be seen from the figure that no WGM resonances were observed in the spectra recorded at the positions along the fiber taper when the waist diameter was $\sim 5 \mu\text{m}$ and larger, indicating that in those cases the power re-coupled from the micro-resonator into the fiber taper due to evanescent field was much lower than that of transmitted power along the fiber taper. At the position corresponding to the diameter of $\sim 3.34 \mu\text{m}$ WGM resonances are observed with a small (0.82 dB) extinction ratio and an overall average spectral loss of -4.34 dB.

As the taper diameter decreases, the extinction ratio of the WGM spectrum gradually improves and the overall transmission loss grows, indicating that more light is coupled into the resonator. When the taper diameter reaches $1.3 \mu\text{m}$, the extinction ratio is 5.43 dB and an average spectral loss is 15.8 dB.

Since in the proposed coupling method involves placing the fiber taper in direct physical contact with the micro-resonator, further decreases in the fiber taper waist diameter beyond $1 \mu\text{m}$ is undesirable as it may result in a fiber taper bend and an associated bend loss, while also being more susceptible to breakage. In our experiments, therefore the fiber taper with the waist diameter of $1.3 \mu\text{m}$, whose SEM image is shown in Figure 5, was employed for light coupling into a 240 μm fiber micro-resonator.

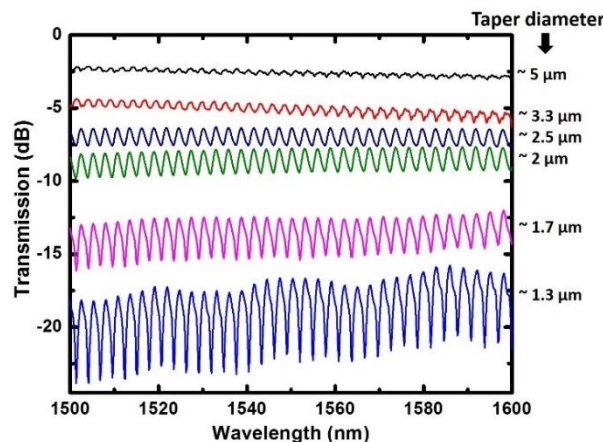


Fig. 4. WGM transmission spectra excited in the cylindrical fiber resonator with a diameter of 240 μm for different tapered fiber diameters.

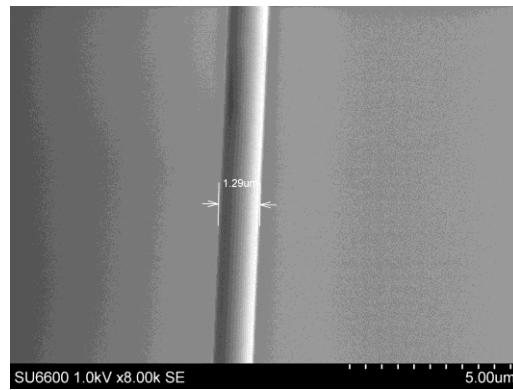


Fig. 5. SEM image of the waist portion of the tapered optical fiber

(d) Dependence of the WGM spectrum on the diameter of the resonator

For the purpose of the experiment, fourteen micro cylinders with different diameters from 8 μm to 125 μm were fabricated from SMF28 fibre using a fiber tapering technique to produce different fiber diameters. Additionally, a single 240 μm micro cylinder was fabricated from a multimode fiber, type BFL 22-200, $\varnothing 240 \mu\text{m}$.

For illustration purposes, Figure 6 (a-d) shows the experimental WGM spectra of different diameter cylindrical micro-resonators excited by the same tapered fiber with the waist diameter of $\sim 1.3 \mu\text{m}$. Figures 6 (a), (b), (c), and (d) show the WGMs spectra for 240 μm , 125 μm , 36 μm , and 8 μm diameter cylindrical silica fiber micro-resonators.

As shown in Figure 6, for a 240 μm diameter cylindrical micro-resonator 34 resonance modes are observed within the range of 1500-1600 nm with an average spectral spacing of 2.89 nm. Decreasing the diameter of the resonator means that the number of modes in a given wavelength range also decreases leading to an increased spectral spacing. The number of modes for cylindrical micro-resonators with diameters of 125 μm , 36 μm and 8 μm are 21, 7, and 2 respectively with corresponding spectral spacings of 4.64 nm, 14.37 nm, and 71 nm. It is noted that the overall transmission loss of the spectrum decreases as the diameter of the micro-resonator reduces.

Figures 7 (a) & (b) illustrates the experimental dependencies of different spectral parameters versus the diameter of the micro-cylinder in the range of diameters from 8 to 240 μm . Figure 7 (a) shows the variation of the FSR of the WGM spectrum versus the resonator diameter. As was shown previously in Figure 6, with a decrease in the diameter of the resonator, the possible number of WGM resonances visible within the specified wavelength range becomes smaller and the spectral separation between the resonance modes increases, consistent with the theory presented earlier.

The widths of the WGM dips increase with the decrease in the size of the resonator. Figure 7 (b) shows the full width at half maximum (FWHM) and Q-factor of selected WGM resonance dips of various cylindrical resonators versus the resonator's diameter. One can see that as the diameter of the resonator decreases, the WGMs resonances broaden. The broadening of the resonance dips is due to the increased curvature loss, and thus a lower Q, when the resonator's diameter becomes smaller.

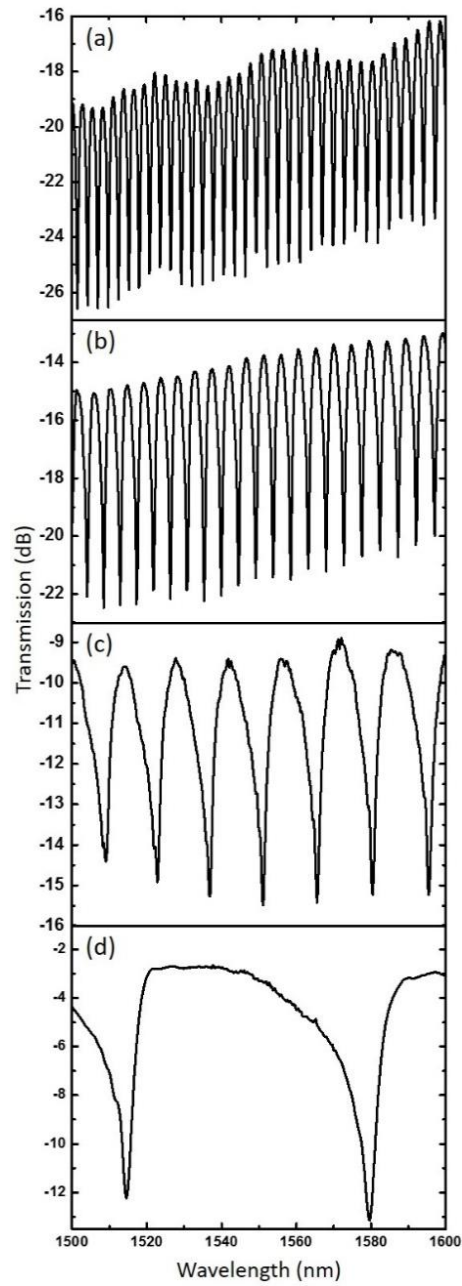


Fig. 6. WGM spectra for cylindrical micro-resonators with different diameters: (a) 240 μm (b) 125 μm (c) 36 μm and (d) 8 μm .

The Q-factor of the WGMs increases with an increase in the diameter of the resonator. In practical experiments, the Q-factor of WGM resonators may be limited by various factors such as irregularities on the surface of the micro-cylinder, losses due to surface contaminants, etc.

Reducing the diameter of the resonator eventually leads to a violation of the total internal reflection (TIR) for the light propagating inside the curved surface of the cavity. Below a certain radius of the cavity, R_{min} the resonator loses its capability to trap light by means of TIR. Considering the WGM path inside a polygon with a side of length λ [36]:

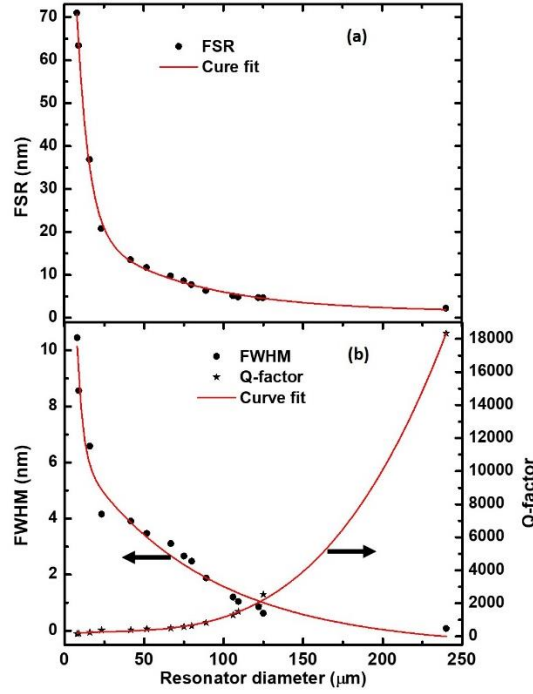


Fig. 7. Variation of (a) free spectral range (FSR), (b) full width at half minimum (FWHM) and quality factor (Q-factor) of the WGM resonances for different diameter resonators with curve fit.

$$R_{\min} = \frac{\lambda}{n_c} \frac{1}{\pi - \theta_{\text{crit}}}, \quad (8)$$

where θ_{crit} (in radian) is the critical angle, n_c is the refractive index of the cavity, and λ is the vacuum wavelength of the circulating light. Using the above equation, one can predict $R_{\min} = 0.45 \mu\text{m}$ by assuming $\lambda = 1550 \text{ nm}$ and $n_c = 1.44$. However, in practical conditions other loss mechanisms add to this fundamental limitation. There are reports on the excitation of WGMs in $1.5 \mu\text{m}$ [36] and $2 \mu\text{m}$ [42] polystyrene micro-spheres. The smallest reported whispering gallery optical resonator is an individual hexagonal ZnO nano-cone whose diameter gradually reduces from bottom to top in the range of 700 to 50 nm and at a wavelength of 380 nm [43]. In our experiments with silica cylindrical micro-resonators we were able to observe WGMs excited in a resonator with a minimum radius of $3 \mu\text{m}$ at a wavelength of 1550 nm .

(e) WGMs in a cylindrical micro-resonator excited by a tilted fiber taper.

Here we present the results of our experimental investigations of WGMs in a cylindrical micro resonator formed by a short length of a multimode fiber, with a diameter of $240 \mu\text{m}$, as a function of the tilt angle of the micro resonator with respect to the fiber taper, used for coupling the light in the resonator. This work is motivated by the need to understand the tolerance of the excitation of WGMs in a cylindrical fiber resonator with respect to changes in the tilt angle.

Figure 8 is a microphotograph of the micro-cylinder tilted from its perpendicular position with respect to the tapered fiber. Here Z_{fiber} is the micro-cylinder axis, creating angle θ (tilt angle) with the laboratory coordinates system $(X_{\text{lab}}, Z_{\text{lab}})$. X_{lab} is the axis of the tapered fiber and Z_{lab} is the normal to the tapered fiber.

As it was shown in the Figure 2, the fabricated fiber taper is straightened and fixed between two translation stages which supports three-dimensional movement for precise alignment. One end of the resonator under test (labeled as “micro-cylinder” in the figure) is fixed on a rotating stage with an angular scale for measurement of the tilt angle and is also mounted on the top of the second translation stage with adjustable vertical position to allow for the light coupling and for an accurate control of the tilt angle between the micro-cylinder and the fiber taper. Due to the short length ($\sim 3 \text{ cm}$) and relatively large diameter of the fiber micro-cylinder it should be noted there is no visible bending of the fiber micro-cylinder observed during the experiment. The choice of a $240 \mu\text{m}$ diameter resonator was used as this has the highest Q-factor and was also the cylinder which suffered the least bending, when supported at one end only.

This process of micro-alignment is repeated for a number of tilt positions of the micro-cylinder with respect to the fiber taper assisted by two optical microscopes, which provide both top and side views of the micro-cylinder-tapered fiber system.

In our experimental setup polarization of the input light was controlled by a three-paddle polarization controller FPC030, with adjustment applied to achieve maximum coupling for a tilt angle of 0° .

Figure 9 (a) shows the transmission spectrum of the fiber taper aligned perpendicularly to the 240 μm diameter fiber cylinder (in the adopted coordinate system this corresponds to $\theta = 0^\circ$).

WGM resonances are clearly present at wavelengths of 1532.55 nm (p1), 1534.84 nm (p2), 1537.09 nm (p3), 1539.38 nm (p4), 1541.67 (p5) and 1544.21 nm (p6). The average extinction ratio, FWHM for the observed resonances and FSR of the spectrum are estimated as 7.76 dB, 0.08 nm and 2.27 nm, respectively. The maximum Q factor is measured as circa 1.83×10^4 . Figure 9 (b) illustrates a selected narrow portion of the experimental spectrum around 1534.8 nm and its Lorentzian fit used to derive the estimated value of the Q factor.

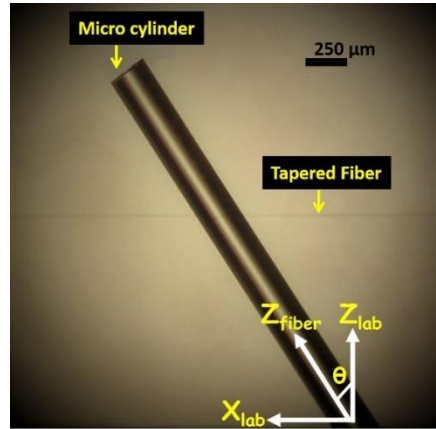


Fig. 8. Microscopic image of the micro-cylinder with the tapered optical fiber.

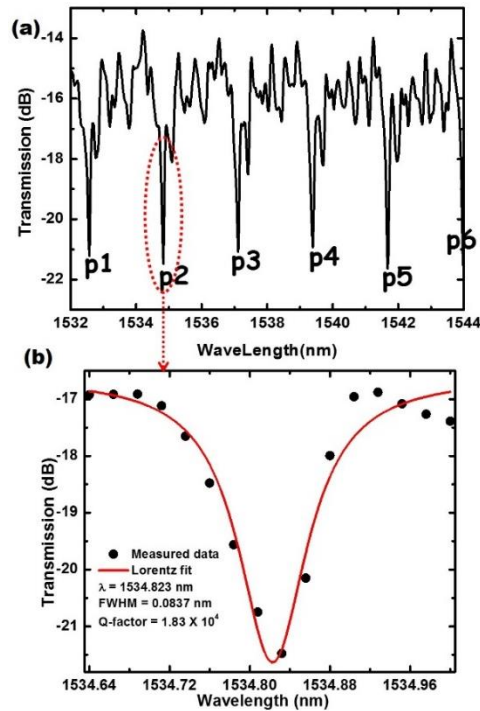


Fig. 9. (a) WGM spectrum generated by a 240 μm diameter cylindrical micro-resonator (normal to the taper, $\theta = 0$). (b) Lorentzian fit of one of the WGM peaks, estimated Q factor is 1.83×10^4 .

The micro-cylinder was then tilted progressively in 2° steps from the perpendicular position to 24° and the spectrum was recorded for each tilt angle. Figure 10 (a) shows the WGM spectra for different tilt angles of the micro cylinder for a representative number of spectra at 0° , 2° , 16° and 20° . Not all of the measured spectra between 0° and 24° are shown in Figure 10 (a) for the sake of clarity.

One can see from the figures that increasing the tilt angle results in an increase in the average loss for the spectrum associated with that tilt angle and the decrease in the extinction ratio for the dips associated with the WGMs. Also some broadening of the WGM resonant dips is observed, accompanied with by a slight blue shift of the dip wavelengths. At tilt angles greater than 24° , no resonance peaks are observed in the measured WGM spectrum.

The observations above could be interpreted as follows: The efficiency of the light coupling from the tapered fiber to a particular WGM inside the micro-cylinder depends on the overlap between the evanescent field of the fiber taper and the corresponding mode field. The overlap is at its maximum when the two fibers are perpendicular to each other. As the tilt angle increases and the micro-cylinder moves away from the perpendicular position ($\theta = 0^\circ$), the fundamental mode field decreases. At the same time with an increase in the tilt angle, the overlap with helical, higher order, WGMs of the resonator improves [13] and as a result coupling into these modes becomes more efficient, which causes the spectral broadening of WGM peaks observed in our experiment.

Figures 10 (b) illustrates the measured variation of the overall average transmission loss of the spectrum and the extinction ratio of the WGMs for different tilt angles. With an increase in the micro resonator tilt angle away from the perpendicular position, the overall average loss of the spectrum increases and a monotonic decrease in the extinction ratio of the WGMs is observed.

It is found that the extinction ratio for the spectral dips reaches a half of its original value in dB when the tilt angle increases to 16° and a quarter of its original value when the tilt angle is equal to 20° . An average reduction of ~ 0.95 dB in the extinction ratio is observed for each 2° increases in the tilt angle.

Finally Figure 10 (c) illustrates the increasing FWHM and the blue shift experienced on a selected WGM resonance dip with an increase in the tilt angle θ . The broadest WGM resonances in our experiment were observed at the tilt angle of 24° with a FWHM greater by 1.6 nm compared with that corresponding to the micro-cylinder which is perpendicular to the fiber taper. The selected WGM dip (p4 in Figure 9 (a)) experienced a 2.6 nm blue shift from the resonance wavelength 1539.38 to 1536.82 nm with the corresponding increase in the tilt angle from 0° to 24° . The significant application of this work is, it is a new method to tune the wavelength and linewidth of WGM of a cylindrical micro-resonator.

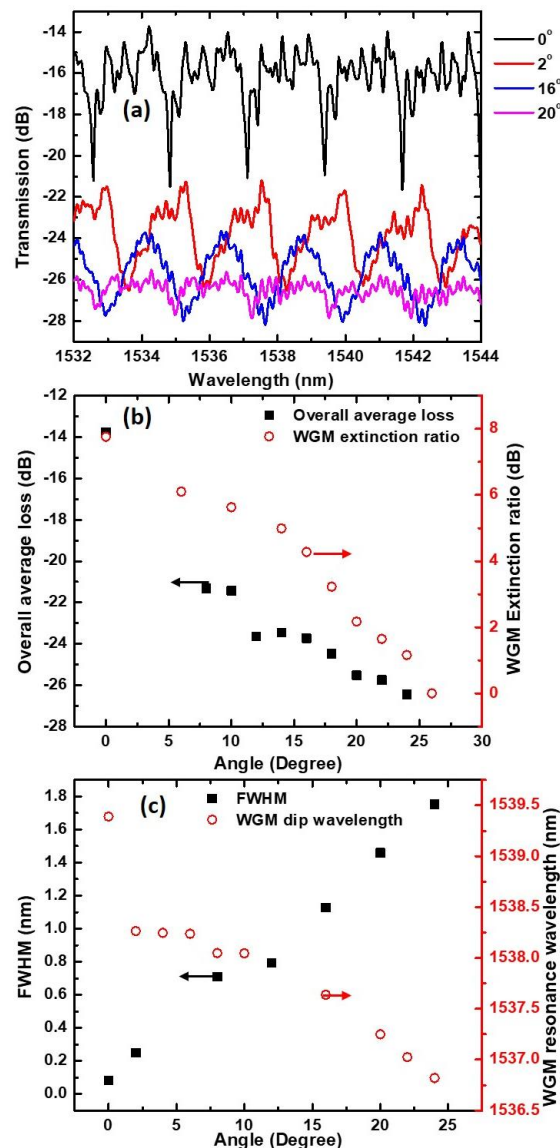


Fig. 10 (a) Transmission spectra of the tapered fiber in contact with the micro-cylinder for different tilt angles with respect to the perpendicular position; (b) overall average loss of the transmission spectrum and extinction ratio of the WGM dip (for peak p2) with the increase in the tilt angle; (c) The broadening of the WGM dip and blue shift experienced on a selected WGM dip with the increase of the tilt angle.

IV. CONCLUSION

In summary, we have experimentally investigated the excitation of WGMs in cylindrical micro-resonators formed by silica optical fibers. The light was evanescently coupled into the micro-cylinder from a tapered optical fiber. The results of our studies allow for experimental determination of the optimum diameter of the tapered optical fiber for efficient evanescent light coupling into the fiber micro-cylinder. The influence of the micro-resonator radius on the WGM spectral parameters, such as the Q-factor and FSR has been experimentally investigated and analyzed. The optimum conditions for generating WGMs in a cylindrical micro-resonator are observed when the tapered fiber is perpendicular to the micro-cylinder. Evolution of the WGM spectrum with the increase of the tilt angle away from its initial perpendicular position resulted in changes in the intensity, broadening and blue shift of the WGM resonant wavelengths. Overall spectral losses increases with the increase of the tilt angle, and a complete disappearance of the WGM resonances occurred at large tilt angles above 24 °.

The results of this work are useful for an understanding of the optimum conditions for excitation of WGMs in cylindrical fiber resonators and can be applied to expand the range of practical applications of cylindrical fiber micro-resonators.

Acknowledgement

Authors would like to acknowledge the support of Dublin Institute of Technology and DIT Fiosraigh Scholarship Program.

REFERENCES

- [1]. G. C. Righini, Y. Dumeige, P. Feron, M. Ferrari, G. Nunzi Conti, D. Ristic and S. Soria, Whispering gallery mode microresonators: Fundamentals and applications, *Rivista Del Nuovo Cimento* **34** (2011), 435-488.
- [2]. A. B. Matsko and V. S. Ilchenko, Optical resonators with whispering gallery modes I: Basics, *IEEE JSTQE* **12** (2006), PP3-14.
- [3]. V. S. Ilchenko and A. B. Matsko, Optical Resonators With Whispering-Gallery Modes—Part II: Applications, *IEEE JSTQE* **12** (2006), 15-32.
- [4]. M. R. Foreman, J. D. Swaim, and F. Vollmer, Whispering gallery mode sensors, *Advances in Optics and Photonics* **7** (2015), 168–240.
- [5]. D. W. Vernooy, V. S. Ilchenko, H. Mabuchi, E. W. Streed, and H. J. Kimble, High-Q measurements of fused-silica microspheres in the near infrared, *Opt. Lett.* **23** (1998), 247-249 .
- [6]. P. Wang, M. Ding, L. Bo, Y. Semenova, Q. Wu and G. Farrell, Packaged chalcogenide microsphere resonator with high Q-factor, *Appl. Phys. Lett.* **102** (2013), 131110-131115.
- [7]. M. Sumetsky, Mode localization and the Q-factor of a cylindrical microresonator, *Opt. Lett.* **14** (2010), 2385-2387.
- [8]. G. Farca, S. I. Shopova and A. T. Rosenberger, Cavity-enhanced laser absorption spectroscopy using microresonator whispering gallery modes, *Opt. Express* **15** (2007), 17443-17448.
- [9]. X. Jin, Y. Dong and K. Wang, Selective excitation of axial modes in a high-Q microcylindrical resonator for controlled and robust coupling, *Appl. Opt.* **54** (2015), 8100-8107.
- [10]. A. W. Poon, R. K. Chang and J. A. Lock, Spiral morphology-dependent resonances in an optical fiber: effects of the fiber tilt and focused Gaussian beam illumination, *Opt. Lett.* **23** (1998), 1105-1107.
- [11]. T. A. Birks, J. C. Knight and T. E. Dimmick, High-resolution measurement of the fiber diameter variations using whispering gallery modes and no optical alignment, *IEEE Photon. Technol. Lett.* **12** (2000), 182-183.
- [12]. M. Sumetsky and Y. Dulashko, Radius variation of optical fibers with angstrom accuracy, *Opt. Lett.* **35** (2010), 4006-4008.
- [13]. A. Boleininger, T. Lake, S. Hami and C. Vallance, Whispering Gallery Modes in Standard Optical Fibres for Fibre Profiling Measurements and Sensing of Unlabelled Chemical Species Sensors **10** (2010), 1765-1781.
- [14]. C. Yin, J. Gu, M. Li, and Y. Song, Tunable high-Q tapered silica microcylinder filter COL 11 (2013), 082302-082305.
- [15]. Xue-Feng Jiang, Yun-Feng Xiao, Qi-Fan Yang, L. Shao, W. R. Clements, and Q. Gong. Free-space coupled, ultralow-threshold Raman lasing from a silica microcavity, *Applied Physics Lett.* **103**, (2013), 10110-10114.
- [16]. Xue-Feng Jiang, Yun-Feng Xiao, Chang-Ling Zou, L. He, Chun-Hua Dong, Bei-Bei Li, Y. Li, Fang-Wen Sun, L. Yang, and Q. Gong, Highly Unidirectional Emission and Ultralow-Threshold Lasing from On-Chip Ultrahigh-Q Microcavities, *Advanced Materials* **24** (2012), OP260-OP264.
- [17]. Qi-Fan Yang, Xue-Feng Jiang, Ya-Long Cui, L. Shao, and Yun-Feng Xiao, Dynamical tunneling-assisted coupling of high-Q deformed microcavities using a free-space beam, *Physical Review A* **88** (2013), 023810-023811.

- [18]. J. C. Knight, G. Cheung, F. Jacques and T. A. Birks, Phase-matched excitation of whispering-gallery-mode resonances by a fiber taper, *Opt. Lett.* **22** (1997), 1129-1131.
- [19]. D. R. Rowland, J. D. Love, Evanescent wave coupling of whispering gallery modes of a dielectric cylinder, *IEEE Proceedings* **140** (1993), 177-188.
- [20]. Y. Panitchob, G. Senthil Murugan, M. N. Zervas, P. Horak, S. Berneschi, S. Pelli, G. Nunzi Conti, and J. S. Wilkinson, Whispering gallery mode spectra of channel waveguide coupled microspheres, *Opt. Express* **16** (2008), 11066-11076.
- [21]. M. L. Gorodetsky and V.S. Ilchenko, High-Q optical whispering -gallery microresonators: precession approach for spherical mode analysis and emission patterns with prism couplers, *Opt. Communications* **113** (1994), 133-143.
- [22]. V. S. Ilchenko, X. S. Yao, and L. Maleki, Pigtailed the high-Q microsphere cavity: a simple fiber coupler for optical whispering-gallery modes, *Opt. Lett.* **24** (1999), 723-725
- [23]. M. Cai, O. Painter, and K. J. Vahala, Observation of critical coupling in a fiber taper to a silica-microsphere whispering-gallery mode system, *Phys. Rev. Lett.* **85** (2000), 74-77.
- [24]. M. J. Humphrey, E. Dale, A. T. Rosenberger and D. K. Bandy, Calculation of optimal fiber radius and whispering-gallery modes spectra for a fiber-coupled microsphere, *Opt. Communications* **271** (2007), 124-131.
- [25]. Y. Dong, K. Wang, and X. Jin, Packaged microsphere-taper coupling system with a high Q factor, *Appl. Opt.* **54** (2015), 277-284.
- [26]. F. Monifi, J. Friedlein, Ş. K. Özdemir, and L. Yang, A robust and tunable add-drop filter using whispering gallery mode microtoroid resonator, *J. Lightwave Technol.* **30** (2012), 3306-3315.
- [27]. F. Monifi, S. K. Özdemir, J. Friedlein, and L. Yang, Encapsulation of a Fiber Taper Coupled Microtoroid Resonator in a Polymer Matrix, *IEEE Photonics Tech. Lett.* **25**, (2013), 1458-1461.
- [28]. G. Zhao, S. K. Ozdemir, T. Wang, L. Xu, E. King, Gui-Lu Long, and L. Yang, Raman lasing and Fano lineshapes in a packaged fiber-coupled whispering-gallery-mode microresonator, *Science Bulletin* **62** (2017), 875- 878
- [29]. F. Bo, S. H. Huang, Ş. K. Özdemir, G. Zhang, J. Xu, and L. Yang, Inverted-wedge silica resonators for controlled and stable coupling, *Opt. Lett.* **39** (2014), 1841-1844.
- [30]. T. Kato, W. Yoshiki, R. Suzuki, and T. Tanabe, Octagonal silica toroidal microcavity for controlled optical coupling, *Appl. Phys. Lett.* **101** (2012), 121101.
- [31]. J. A. Lock, Scattering of a diagonally incident focused Gaussian beam by an infinitely long homogeneous circular cylinder, *JOSA A* **14** (1997), 640-652.
- [32]. J. A. Lock, Morphology-dependent resonances of an infinitely long circular cylinder illuminated by a diagonally incident plane wave or a focused Gaussian beam, *JOSA A* **14** (1997), 653-661.
- [33]. D. G. Rabus, *Integrated Ring Resonators*, Springer series in Optical Sciences, Springer, USA, 2007, pp.3-40.
- [34]. W. Bogaerts, P. D. Heyn, T. V. Vaerenbergh, K. DeVos, S. K. Selvaraja, T. Claes, P. Dumon, P. Bienstman, D. Van Thourhout, and R. Baets, Silicon microring resonators, *Laser Photonics. Rev.* **6** (2012), 47-73.
- [35]. W. Lin, H. Zhang, B. Liu, B. Song, Y. Li, C. Yang and Y. Liu, Laser-tuned whispering gallery modes in a solid-core microstructured optical fibre integrated with magnetic fluids, *Nat. Sci. Rep.* **5** (2015), 17791.
- [36]. A. Weller, F. C. Liu, R. Dahint, M. Himmelhaus, Whispering gallery mode biosensors in the low-Q limit, *Appl. Phys. B* **90** (2008), 561-567.
- [37]. M. L. Gorodetsky, A. A. Savchenkov, and V. S. Ilchenko, Ultimate Q of optical microsphere resonators, *Opt. Lett.* **21** (1996), 453-455.
- [38]. M. Ahmad, L. L. Hench, Effect of taper geometries and launch angle on evanescent wave penetration depth in optical fibers, *Biosensors and Bioelectronics* **20** (2005), 1312-1319.
- [39]. K. R. Harper, T. E. Dimmick, and T. E. Dubroff, Tapered optical fibers, U.S. Patent Application No. 11/473,689.
- [40]. M. Sumetsky, How thin can a microfiber be and still guide light?, *Opt. Lett.* **31** (2006), 870-872.
- [41]. G. Brambilla, V. Finazzi, and D. Richardson, Ultra-low-loss optical fiber nanotapers, *Opt. Express.* **12** (2004), 2258-2263.
- [42]. T. Mukaiyama, K. Takeda, H. Miyazaki, Y. Jimba, M. Kuwata-Gonokami, Tight-binding photonic molecule modes of resonant bispheres, *Phys. Rev. Lett.* **82** (1999), 4623.
- [43]. Y. H. Yang, Y. Zhang, N. W. Wang, C. X. Wang, B. J. Li and G. W. Yang, ZnO nanocone: Application in fabrication of the smallest whispering gallery optical resonator, *Nanoscale* **3** (2011), 592-597.